Hindawi Publishing Corporation
International Journal of Photoenergy
Volume 2013, Article ID 823254, 8 pages
http://dx.doi.org/10.1155/2013/823254

Research Article

Effectively Improved SiO_2-TiO_2 Composite Films Applied in Commercial Multicrystalline Silicon Solar Cells

Chih-Hsiang Yang,[1] Shui-Yang Lien,[2] Chia-Ho Chu,[3] Chung-Yuan Kung,[1] Tieh-Fei Cheng,[4] and Pai-Tsun Chen[4]

[1] *Department of Electrical Engineering, National Chung Hsing University, Taichung, Taiwan*
[2] *Department of Materials Science and Engineering, DaYeh University, ChungHua, Taiwan*
[3] *Department of Materials Science and Engineering, MingDao University, 369 Wen-Hua Road, Peetow, ChungHua 52345, Taiwan*
[4] *Gallant Precision Machining Co., Ltd., Taichung, Taiwan*

Correspondence should be addressed to Shui-Yang Lien; syl@mail.dyu.edu.tw

Received 14 June 2013; Accepted 13 August 2013

Academic Editor: Gaetano Di Marco

Composite silicon dioxide-titanium dioxide (SiO_2-TiO_2) films are deposited on a large area of 15.6 × 15.6 cm^2 textured multicrystalline silicon solar cells to increase the incident light trapped within the device. For further improvement of the antireflective coatings (ARCs) quality, dimethylformamide (DMF) solution is added to the original SiO_2-TiO_2 solutions. DMF solution solves the cracking problem, thus effectively decreasing reflectance as well as surface recombination. The ARCs prepared by sol-gel process and plasma-enhanced chemical vapor deposition (PECVD) on multicrystalline silicon substrate are compared. The average efficiency of the devices with improved sol-gel ARCs is 16.3%, only 0.5% lower than that of devices with PECVD ARCs (16.8%). However, from equipment depreciation point of view (the expiration date of equipment is generally considered as 5 years), the running cost (USD/watt) of sol-gel technique is 80% lower than that of PECVD method for the first five years and 66% lower than that of PECVD method from the start of the sixth year. This result proves that sol-gel-deposited ARCs process has potential applications in manufacturing low-cost, large-area solar cells.

1. Introduction

Antireflective coatings (ARCs) are now widely used in mass produced silicon photovoltaics [1–3]. High quality ARCs must be designed accurately on mono- and multicrystalline silicon solar cell surfaces, not only to passivate the surface dangling bonds acting as recombination centers [4–8], but also to minimize the loss of optical absorption. The conventional plasma-enhanced chemical vapor deposition (PECVD) technique is employed generally to deposit antireflection layers such as Si_3N_4 and SiO_2 [9–13]. However, this technique is always associated with vacuum processes and dangerous process gases. Therefore, replacing PECVD by other cost-effective methods can considerably reduce production costs of manufacturers and raise the security of the clean-room environment. Sol-gel spin-coating method applied extensively in preparing lots of different kinds of coated films has become a popular technique for the past thirty years due to its high process speed, low-cost, continuous production, and suitability for the large-area process [14–17]. Nevertheless, ARCs deposited on textured silicon wafers by sol-gel method present worse uniformity than those deposited by PECVD technique. The severest nonuniformity areas resulting from centrifugal force appear on four corners of the substrate. For overcoming it, we control the spin rate of the spin coater, spin duration, and adjust the concentration of sol-gel solutions. Further, adding dimethylformamide (DMF) solution to the composite films is a critical step to solve the problem of film cracking. Mostly, cracks are caused owing to different coefficients of thermal expansion between the air and ARCs films [18–20]. Although the basic properties of most kinds of sol-gel-deposited films have been discussed, the application of composite films in solar cell research is not well investigated.

This study proposes a simple low-cost sol-gel method of preparing high-quality ARCs on large area multicrystalline wafers. DMF solution can help ARCs to be effectively coated on irregular and rough wafer surfaces treated by acid texturing. The average efficiency of solar cells with sol-gel-deposited antireflective films approaches that of ready-made crystalline solar cells. Thus, using sol-gel method instead of PECVD technique to deposit ARCs has potential applications in mass production of solar cells.

2. Experiment

2.1. Preparation of Sol-Gel Solution and Process of Spin Coating. The experimental SiO_2-TiO_2 colloid solutions in this study contained varying volume ratios of SiO_2 and TiO_2 solutions. The SiO_2 solution was prepared by reacting metal alkoxide with a mixture of a critical amount of water and hydrochloric acid (HCl) catalyst in a medium diluted with ethyl alcohol solvent. Tetraethyl orthosilicate ($Si(OC_2H_5)_4$) was then added into the resultant solutions and stirred with a magnetic stirrer. The TiO_2 solution was prepared similarly except that titanium isopropoxide ($Ti(OC_3H_9)_4$) was added instead of ($Si(OC_2H_5)_4$). The SiO_2 and TiO_2 were then mixed separately in different volume ratios. Tables 1, 2, and 3 show the detailed information for all solutions. Finally, a small amount of DMF was added into the SiO_2-TiO_2 synthetic colloid solution.

After adding several drops of synthetic solution to the $15.6 \times 15.6\,cm^2$ multicrystalline wafers, the wafers were spin-coated for two rounds. The first coating was applied at a speed of 150 rpm to ensure uniform composite films, and the second round was performed at 330 rpm to obtain the desired film thickness. Each film was then prebaked at 80°C for 20 min and postbaked at 200°C for 40 min in atmosphere. Then, samples were further annealed in a quartz furnace from 100°C to 850°C for around 30 seconds firstly. Then furnace temperature cooled down from 850°C to around 100°C and lasted for 30 seconds.

Optical characteristics such as refractive index, thickness, and reflectance of films were subsequently measured by ellipsometer and fiber coupled CCD array spectrometer, respectively.

2.2. Design of Antireflection Coatings. More incident light is essential for mono- and multicrystalline solar cells to enhance their short-circuit current (J_{sc}). In some applications, zero reflectance is needed throughout a narrow spectrum band or at a single wavelength. For a substrate with a single ARC, the light from the ARC-substrate interface is reflected back to the ambient (air)-ARC interface with a phase change of 180° and interfere with the light reflected from the interface between ambient (air) and ARC in the opposite direction. In this state, the reflectance R can be described as

$$R = \left[\frac{n_{ARC}^2 - n_0 n_{sub}}{n_{ARC}^2 + n_0 n_{sub}}\right]^2, \quad (1)$$

Table 1: Preparation of SiO_2 solution.

Contents	Ratio	Adding order
H_2O/HCl	0.2/0.0005	1
C_2H_5OH	0.5	2
$Si(OC_2H_5)_4$	0.05	3

Table 2: Preparation of TiO_2 solution.

Contents	Ratio	Adding order
H_2O/HCl	1	1
C_2H_5OH	80	2
$Ti(OC_3H_9)_4$	1	3

Table 3: Preparation of mixed SiO_2-TiO_2 solution.

Contents	Notation
Ratio of SiO_2 to TiO_2	0.05~10
Coating rate (r.p.m)	100~400
DMF ($(CH_3)_2NCHO$) (%)	0~20

where n_{ARC}, n_0, and n_{sub} are the refractive indices of the ARC material, air, and substrate, respectively. To obtain zero reflectance, the term of $n_{ARC}^2 - n_0 n_{sub}$ must be zero. The resulting boundary condition can then be described as

$$n_{ARC} = \sqrt{n_0 n_{sub}}. \quad (2)$$

Moreover, the optimum thickness and refractive index with a minimum reflectance for a single-layer ARC can be deduced from

$$\lambda_0 = 4 n_{ARC} d_{ARC}, \quad (3)$$

where λ_0 is the midrange wavelength of 630 nm, and where n_{ARC} and d_{ARC} are the refractive index and layer thickness, respectively [21].

2.3. Solar Cell Performance. Solar cells were fabricated from boron-doped multicrystalline Si wafers with resistivity of approximately 15 Ω-cm. Wafers were textured using hydrofluoric acid. After forming the emitter region by thermal diffusion of phosphorous atoms in a quartz tube furnace at 850°C, the back surface field was formed by annealing the aluminum contact deposited using screen printing method. The composite SiO_2-TiO_2 films and Si_3N_4 films were then deposited on the front of solar cells by spin-coating and PECVD techniques, respectively. Quasi-Steady-State Photoconductance lifetime measurement technique (QSSPC) was carried out to evaluate the surface passivation effect of the ARCs on silicon substrate. Front silver contact prepared through screen printing method was then annealed at 700°C for 30 min. Finally, effective illuminated light (AM 1.5 G) from the solar simulator was slightly decreased by the grid-type collecting electrode, which occupied about 8% of the front surface area.

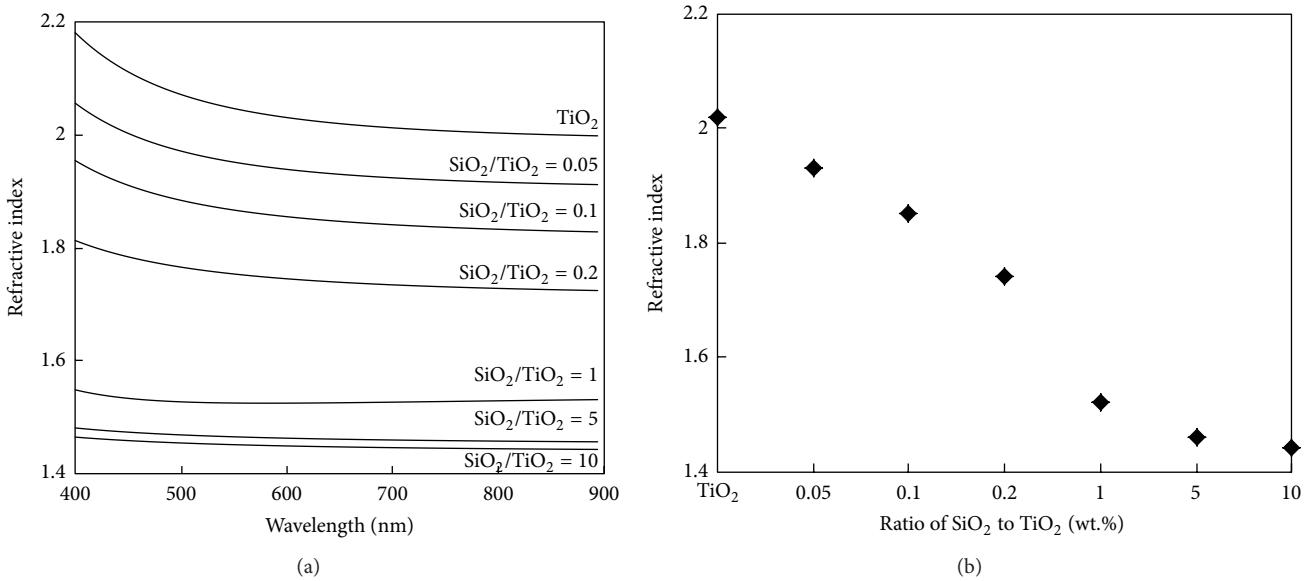

(a) (b)

Figure 1: (a) Refractive index spectra and (b) refractive index at 630 nm for pure TiO_2 and SiO_2-TiO_2 composite films deposited on monocrystalline substrates.

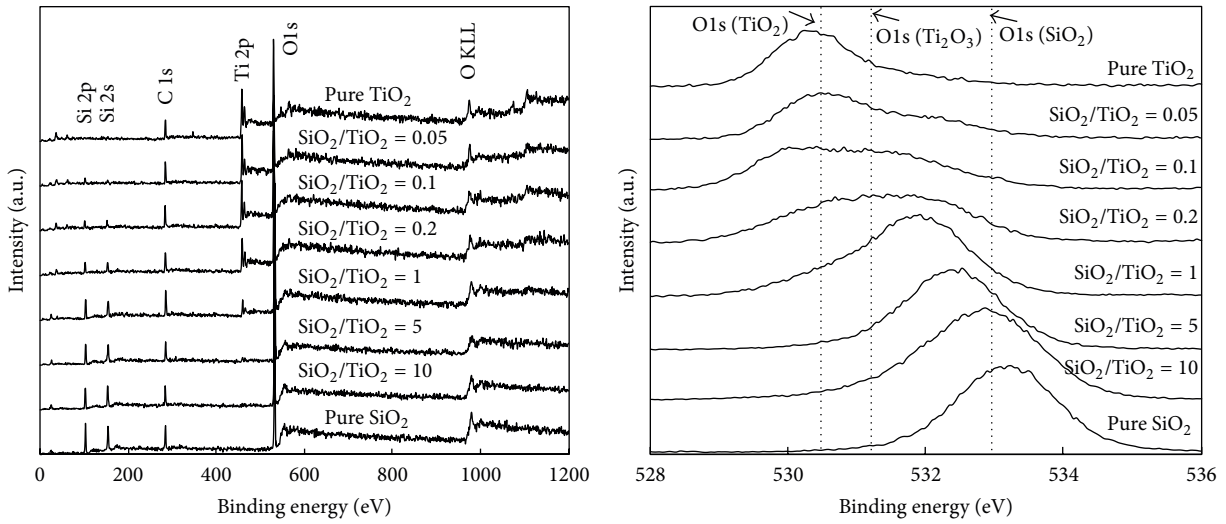

(a) (b)

Figure 2: (a) XPS spectra and (b) O1s spectra for different ratios of SiO_2-TiO_2 composite films.

3. Results and Discussion

When designing an ARC, the goal is to determine the refractive index and thickness of SiO_2-TiO_2 films that provide optimal performance along the desired spectrum. Figure 1(a) shows refractive index spectra for pure TiO_2 and SiO_2-TiO_2 composite films deposited on monocrystalline substrates. The average refractive index is defined as the average value of all points on each curve. It can be found that as the pure TiO_2 solution adds more volumes of SiO_2 solution, the average refractive index decreases obviously from 2.1 to 1.45. Figure 1(b) further shows the different refractive indices corresponding to each ratio of SiO_2 to TiO_2 (SiO_2/TiO_2) at a wavelength of 630 nm. At this wavelength, spectral photon intensity is the highest, and the strongest destructive interference happens, causing light to be trapped in devices [21]. Based on the boundary condition equation (2) mentioned previously, the appropriate refractive index 1.85 is obtained while the SiO_2/TiO_2 ratio is 0.1.

For analyzing the properties of composite films, X-ray photoelectron spectroscopy (XPS) spectra for pure SiO_2 film, pure TiO_2 film, and their mixture films in different SiO_2/TiO_2 ratios is carried out within the binding energy of 0–1200 eV as shown in Figure 2(a). The Si 2p, Si 2s, Ti 2p, and O 1s binding energy locate at 103.1, 155, 456.6, and 532.4 eV, respectively. The C 1s peak is 284.7 eV, which is attributable to carbon contamination at the outer surface of the composite films. The Ti 2p peaks gradually disappear with increasing of

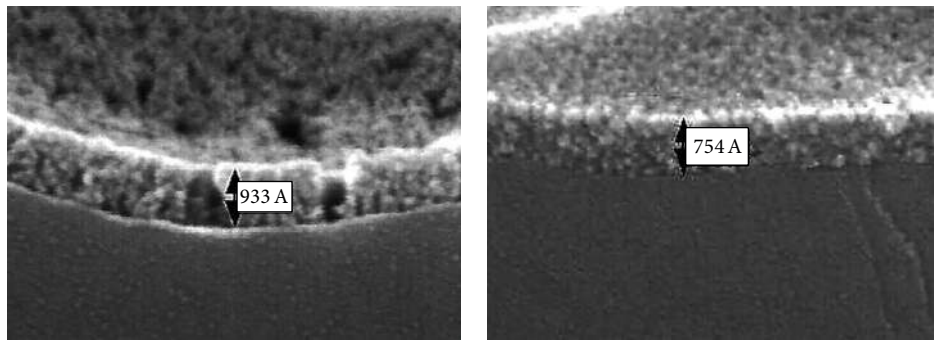

(a) Before annealing (b) After annealing

Figure 3: Cross-sectional SEM images (a) before firing and (b) after firing of SiO_2-TiO_2 composite films.

SiO_2/TiO_2 ratio, whereas the Si 2s and Si 2p peaks strengthen, which validates that the components of all composite films changed momentarily. Figure 2(b) shows the results of further analysis of the behaviors of O 1s peaks in composite films with various SiO_2/TiO_2 ratios. The peak shifts from low binding energy (Ti–O bonds) to high binding energy (Si–O bond). Characteristics of composite film get close to that of pure SiO_2 film. From the materials analysis perspective, these changes explain why the refractive index of SiO_2-TiO_2 composite films changes as different SiO_2/TiO_2 ratios.

Since the ratio of SiO_2/TiO_2 has been optimized to 0.1, we start to investigate the properties of composite films based on this ratio in later experiment. Figure 3 is a scanning electron microscope (SEM) cross-sectional image of the SiO_2-TiO_2 composite films before and after annealing process. It can be seen in Figure 3(a) that, by adjusting spinning speed, the SiO_2-TiO_2 composite film can be coated to the surface of textured multicrystalline wafer smoothly, but is still loose before annealing. After annealing at 850°C for 30 seconds, thickness of ARC decreases from 93.3 nm to 75.4 nm as shown in Figure 3(b). The film becomes denser, probably attributed to firing of the organic solvent and removal of resin [22]. However, in this case, a desirable thickness approximating 85 nm is calculated using (3) shown previously. A 10 nm deviation exists between theoretical value and experimental result, leading to a very slight influence on cell's performance. It's really difficult to control the film thickness accurately of using sol-gel technique; therefore, how to improve this disadvantage is a critical issue in the future.

The SEM images of surface morphology of composite SiO_2-TiO_2 films with DMF ranging from 0% to 15% are schematically presented in Figure 4. Figure 4(a) exhibits lots of cracks in the composite SiO_2-TiO_2 film without DMF. From the zoomed insert, visible cracks spread on the bottom of notches formed by acid texturing. The cracks, which probably formed during the annealing process, decrease the absorption of incident photons. Worse light absorption may lead to lower light-generated carriers, thus decreasing the J_{sc} of solar devices. Figures 4(b) to 4(d) show that adding 5% to 15% DMF to SiO_2-TiO_2 solutions gradually improves the crack problems. When the DMF ratio reaches 15%, the cracks are almost entirely eliminated. This phenomenon may be probably explained that DMF solution can not only diminish the reaction rate of sol hydrolyzing-polycondensation and prevent the little sol particle from growing up, but also promotes the lateral connection of particles by combining the hydrogen bonds with intermediates of sol during gelling process. Moreover, the pore tension of mixture solution could be diminished by DMF solution in thermal process, leading to lower vapor pressure. Hence, the composite films are coated uniformly. According to QSSPC measurement (not shown here), the lifetime of excess minor carrier of each composite film with 0% to 15% DMF solution are 2, 8, 17, and 23 μs, respectively, revealing that as the cracks in the films reduce, the lifetimes becomes higher. Compared to the lifetime of monocrystalline silicon substrate, these relative low lifetime values can be attributed to lots of grain boundaries in multicrystalline silicon substrate, which act as recombination centers.

Figure 5 displays the optical reflectance spectra of pure TiO_2 films, SiO_2-TiO_2 composite films with different volume of DMF, and Si_3N_4 films fabricated by PECVD. The results show that the PECVD ARC has a higher reflectance compared to other films prepared by sol-gel technique at wavelengths lower than 500 nm. This relatively high value is attributed to its relatively higher refractive index of Si_3N_4 at short wavelength [16]. The PECVD ARC has an average reflectance of approximately 9.5%, and its minimum reflectance is approximately 1.5% at wavelengths approximating 770 nm. Further comparison of the curves of the other composite films with and without DMF shows that lowest average reflectance is obtained while the mixed SiO_2-TiO_2 solution plus 15% DMF, presenting an average reflectance of 9% and minimum reflectance of approximately 4% at the wavelength around 670 nm. Obviously, composite films without cracks provide suitable path for incident light, reducing the reflection loss considerably. In summary, the entire measured tendency corresponds well with the SEM images shown in Figure 4, revealing the feasibility of adding DMF solution.

Figure 6 compares performances of solar cells between PECVD-ARC cells (ready-made multicrystalline cells for mass production) and improved sol-gel-ARC cells. All performance parameters for the fifty devices with optimal sol-gel

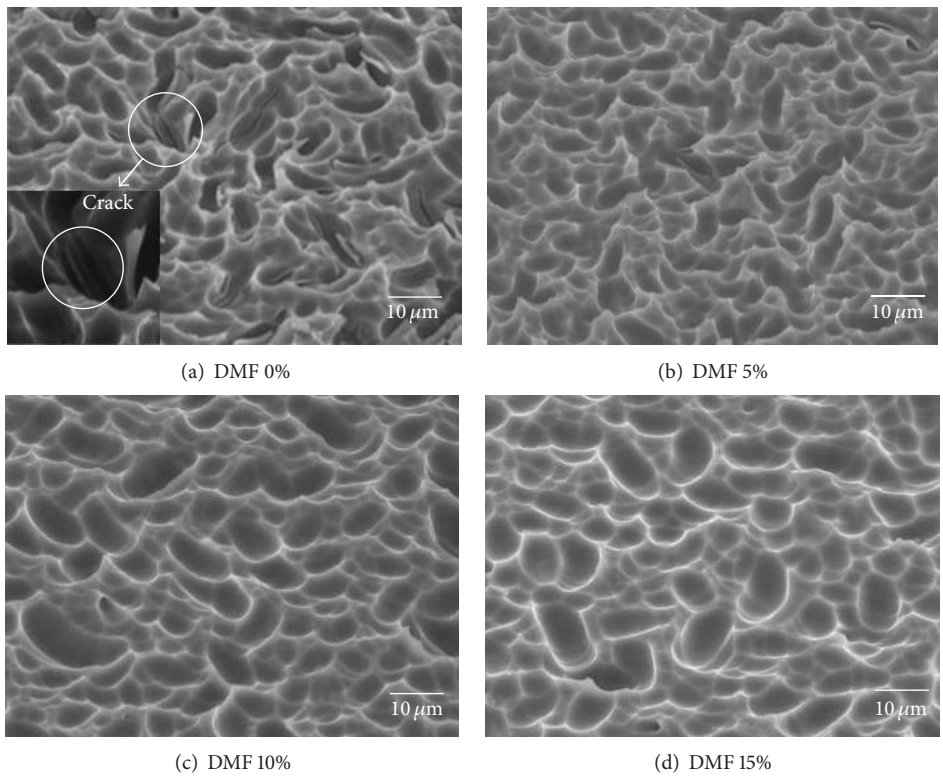

(a) DMF 0% (b) DMF 5%

(c) DMF 10% (d) DMF 15%

Figure 4: SEM images of surface morphology of composite SiO_2-TiO_2 films without DMF and with DMF ratios from 5% to 15%.

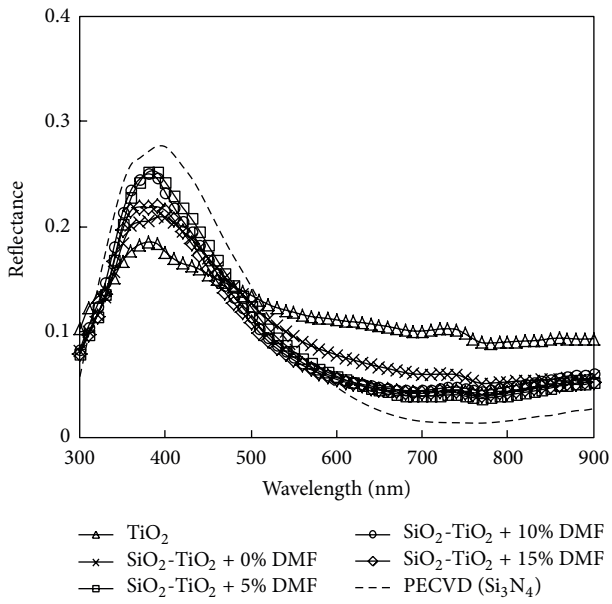

Figure 5: Optical reflectance spectra of pure TiO_2 film, SiO_2-TiO_2 mixture films with different volumes of DMF, and Si_3N_4 films fabricated by PECVD.

ARCs are highly consistent, which confirms the reliability of the process. The optimum average efficiency is approximately 16.3%, about 0.5% lower than the average efficiency (around 16.8%) of PECVD-ARC cells. This 0.5% discrepancy is caused mainly by short-circuit current and open-circuit voltage (V_{oc}). The chief reason of the lower J_{sc} of those sol-gel-ARCs devices can be discussed in two factors: reflectance and lifetime. As noted in Figure 5, the average reflectance of sol-gel-ARCs devices plus 15% DMF solution is 9%, which is lower than 9.5% of the PECVD-ARCs devices. It is expected that sol-gel-ARC device should absorb more incident light resulting in higher J_{sc}. However, average J_{sc} of the sol-gel-ARCs devices is 34.9 lower than 35.2 mA/cm^2 of the PECVD-ARC devices, which implies that the carrier lifetime substantially affects J_{sc}. Noted that the mean lifetime of PECVD-ARCs devices is around 27 μs and of the sol-gel-ARCs devices is around 23 μs. Moreover, lower mean lifetime of the sol-gel-ARCs devices also affects their V_{oc} performance. Michl et al. indicated that the excess minor carrier lifetime substantially affects the V_{oc} in multicrystalline devices [23]. This result is consistent with the experimental trend in this study. Hence, further studies are needed to improve the interface quality between a sol-gel-ARC and a silicon substrate.

Figure 7 compares the appearance of a PECVD-ARC device (Figure 7(a)) with a sol-gel-ARC device (Figure 7(b)). Before fabrication of the ARCs, both devices initially have the same multicrystalline silicon substrates. It can be seen that the colors of both devices are nearly the same after fabricating ARCs. Very little color variation is caused by the different reflectance of both devices at visible wavelength spectrum. The deep blue sol-gel-ARC is quite uniform without any uncoated areas formed on the four corners of the substrate, indicating that the proposed sol-gel process can potentially

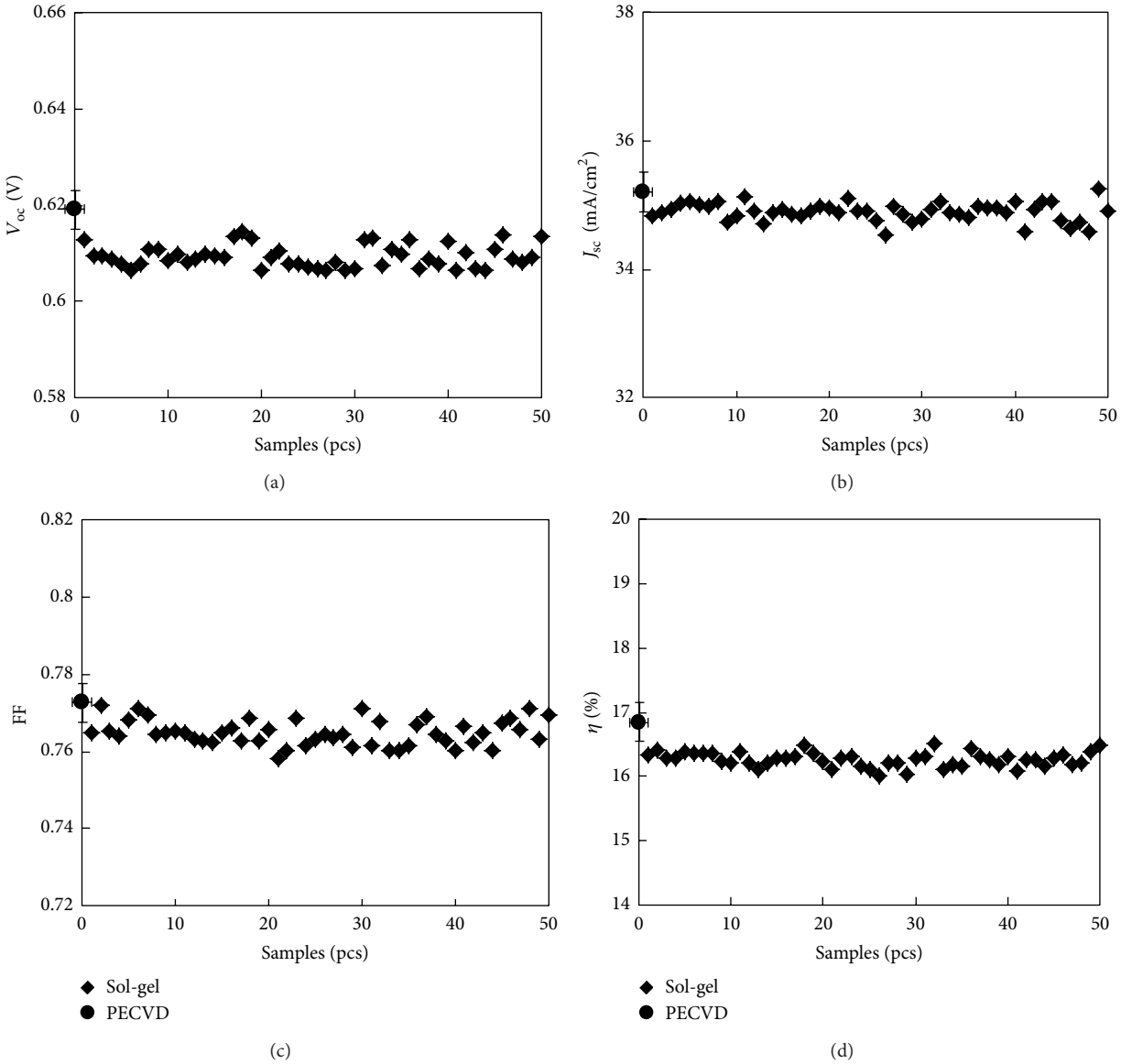

Figure 6: Performances of the PECVD-ARC solar cells and the sol-gel-ARC solar cells.

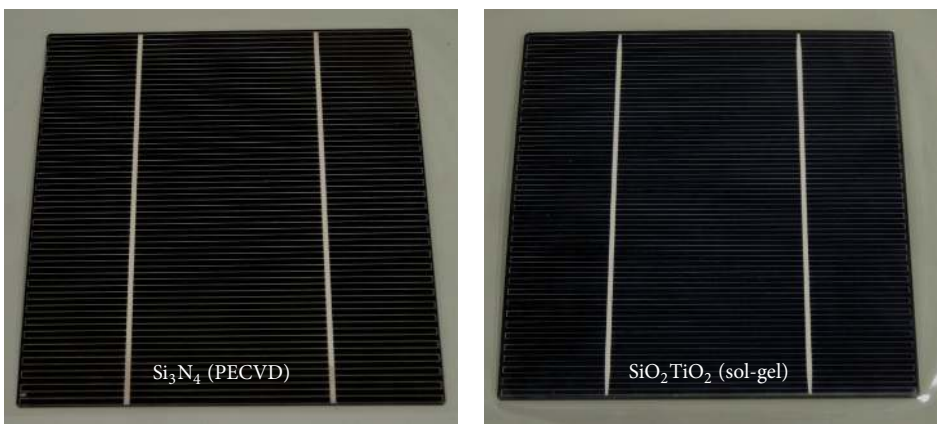

Figure 7: Photographs of (a) PECVD-ARC device and (b) sol-gel-ARC devices.

Table 4: Cost in fabricating ARCs.

Cost in ARC process (USD)	PECVD (Si_3N_4)	Spin-coating (SiO_2-TiO_2)
Equipments	1,040,000	33,333
Materials (1 year)	407,000	121,300
Running cost/Per Watt (first five years)	0.0154	0.003
Running cost/Per Watt (five years later)	0.01	0.003

replace the PECVD process for the mass production of single- and multicrystalline silicon solar cells.

Table 4 provided by Gallant Precision Machining Co., Ltd., Taiwan compares equipment cost, materials cost, and running cost between various ARCs fabrication methods. The expiration date of equipment is generally considered as five years. From equipment depreciation point of view, the running cost (USD/watt) of sol-gel technique is around 80% lower than that of PECVD method for first five years and around 66% lower than that of PECVD method from the start of the sixth year. Although the efficiency of sol-gel-ARC device is lower than that of PECVD-ARC device, a huge difference in manufacturing cost still makes sol-gel-ARC device have enough competitiveness.

For further increasing efficiency of the proposed sol-gel-ARCs cells, it is necessary to fabricate double or even triple layers ARCs. A single layer ARC is able to be nonreflective only at one wavelength, often at the middle of the visible region, but multiple layers are more effective over the whole visible spectrum. Moreover, high conversion efficiency of monocrystalline silicon solar cells can probably be realized with the same sol-gel process.

4. Conclusion

A study aiming to improve the quality of sol-gel ARCs that could help increase the efficiency of multicrystalline solar cells is presented in this work. The effective refractive index and thickness of the films are adjusted by controlling the spin rate and annealing temperature. Average reflectance is eventually reduced to 9% by adding DMF solution to reduce cracks in the film while the average efficiency of devices is improved to 16.3%. Although the efficiency 16.3% still trails that of the ready-made multicrystalline solar cells by approximately 0.5%, the reliability and uniformity as well as lower running cost are highly attractive to manufacturers. In the future, use of the sol-gel technique, which combines spin-coating with furnace annealing to prepare ARCs, could enable a more efficient and a continuous mass production of Si solar cells compared to the use of PECVD method, which requires an expensive vacuum process and dangerous process gases.

Acknowledgments

This work is sponsored by Gallant Precision Machining Co., Ltd., Taiwan and the National Science Council of Taiwan under the Grants nos. NSC 100-2628-E-451-002-MY2(2/2) and NSC 101-3113-E-451-001-CC2.

References

[1] S.-M. Jung, Y.-H. Kim, S.-I. Kim, and S.-I. Yoo, "Design and fabrication of multi-layer antireflection coating for III-V solar cell," *Current Applied Physics*, vol. 11, no. 3, pp. 538–541, 2011.

[2] S. Duttagupta, F. Ma, B. Hoex, T. Mueller, and A. G. Aberle, "Optimised antireflection coatings using silicon nitride on textured silicon surfaces based on measurements and multidimensional modelling," *Energy Procedia*, vol. 15, pp. 78–83, 2012.

[3] J. H. Selj, T. T. Mongstad, R. Søndenå, and E. S. Marstein, "Reduction of optical losses in colored solar cells with multilayer antireflection coatings," *Solar Energy Materials and Solar Cells*, vol. 95, no. 9, pp. 2576–2582, 2011.

[4] H. J. Yang, K.-S. Ji, J. Choi, and H. M. Lee, "Annealing effect on surface passivation of a-Si:H/c-Si interface in terms of crystalline volume fraction," *Current Applied Physics*, vol. 10, no. 3, pp. S375–S378, 2010.

[5] J. W. A. Schüttauf, C. H. M. V. der Werf, W. G. J. H. M. van Sark, J. K. Rath, and R. E. I. Schropp, "Comparison of surface passivation of crystalline silicon by a-Si:H with and without atomic hydrogen treatment using hot-wire chemical vapor deposition," *Thin Solid Films*, vol. 519, no. 14, pp. 4476–4478, 2011.

[6] T. C. Thi, K. Koyama, K. Ohdaira, and H. Matsumura, "Passivation characteristics of SiN_x/a-Si and SiN_x/Si-rich-SiN_x stacked layers on crystalline silicon," *Solar Energy Materials and Solar Cells*, vol. 100, pp. 169–173, 2012.

[7] T. F. Schulze, L. Korte, and B. Rech, "Impact of a-Si:H hydrogen depth profiles on passivation properties in a-Si:H/c-Si heterojunctions," *Thin Solid Films*, vol. 520, no. 13, pp. 4439–4444, 2012.

[8] J. Ge, Z. P. Ling, J. Wong, T. Mueller, and A. G. Aberle, "Optimisation of intrinsic a-Si:H passivation layers in crystalline-amorphous silicon heterojunction solar cells," *Energy Procedia*, vol. 15, pp. 107–117, 2012.

[9] J. Ko, D. Gong, K. Pillai et al., "Double layer SiN_x:H films for passivation and anti-reflection coating of c-Si solar cells," *Thin Solid Films*, vol. 519, no. 20, pp. 6887–6891, 2011.

[10] W. R. Taube, A. Kumar, R. Saravanan et al., "Efficiency enhancement of silicon solar cells with silicon nanocrystals embedded in PECVD silicon nitride matrix," *Solar Energy Materials and Solar Cells*, vol. 101, pp. 32–35, 2012.

[11] S. Wang, A. Lennon, B. Tjahjono, L. Mai, B. Vogl, and S. Wenham, "Overcoming over-plating problems for PECVD SiN_x passivated laser doped p-type multi-crystalline silicon solar cells," *Solar Energy Materials and Solar Cells*, vol. 99, pp. 226–234, 2012.

[12] R. Bousbih, W. Dimassi, I. Haddadi, S. Ben Slema, P. Rava, and H. Ezzaouia, "Silicon lifetime enhancement by SiN_x:H anti-reflective coating deposed by PECVD using SiH_4 and N_2 reactive gas," *Solar Energy*, vol. 86, no. 5, pp. 1300–1305, 2012.

[13] L. Remache, E. Fourmond, A. Mahdjoub, J. Dupuis, and M. Lemiti, "Design of porous silicon/PECVD SiO_x antireflection coatings for silicon solar cells," *Materials Science and Engineering B*, vol. 176, no. 1, pp. 45–48, 2011.

[14] G. Guzman, B. Dahmani, J. Puetz, and M. A. Aegerter, "Transparent conducting sol-gel ATO coatings for display applications by an improved dip coating technique," *Thin Solid Films*, vol. 502, no. 1-2, pp. 281–285, 2006.

[15] J. Puetz and M. A. Aegerter, "Dip coating technique," in *Handbook on Sol-Gel Technologies for Glass Producers and Users*, M. A. Aegerter and M. Mennig, Eds., p. 37, Kluwer Academic Publishers, 2004.

[16] M. Vishwas, K. N. Rao, K. V. A. Gowda, and R. P. S. Chakradhar, "Optical, electrical and dielectric properties of TiO_2-SiO_2 films prepared by a cost effective sol-gel process," *Spectrochimica Acta A*, vol. 83, no. 1, pp. 614–617, 2011.

[17] N. H. Aljufairi, "Electric properties and surface structure of TiO_2 for solar cells," *Energy*, vol. 39, no. 1, pp. 6–10, 2012.

[18] Z. Zhang, P. Zhang, L. Guo, T. Guo, and J. Yang, "Effect of TiO_2-SiO_2 sol-gel coating on the cpTi-porcelain bond strength," *Materials Letters*, vol. 65, no. 7, pp. 1082–1085, 2011.

[19] Ö. Kesmez, E. Burunkaya, N. Kiraz, H. E. Çamurlu, M. Asiltürk, and E. Arpaç, "Effect of acid, water and alcohol ratios on sol-gel preparation of antireflective amorphous SiO_2 coatings," *Journal of Non-Crystalline Solids*, vol. 357, no. 16-17, pp. 3130–3135, 2011.

[20] A. Elfanaoui, E. Elhamri, L. Boulkaddat et al., "Optical and structural properties of TiO_2 thin films prepared by sol-gel spin coating," *International Journal of Hydrogen Energy*, vol. 36, no. 6, pp. 4130–4133, 2011.

[21] T. Mizuta, T. Ikuta, T. Minemoto, H. Takakura, Y. Hamakawa, and T. Numai, "An optimum design of antireflection coating for spherical silicon solar cells," *Solar Energy Materials and Solar Cells*, vol. 90, no. 1, pp. 46–56, 2006.

[22] N. Batra, P. Kumar, S. K. Srivastava et al., "Controlled synthesis and characteristics of antireflection coatings of TiO_2 produced from a organometallic colloid," *Materials Chemistry and Physics*, vol. 130, no. 3, pp. 1061–1065, 2011.

[23] B. Michl, M. Rüdiger, J. A. Giesecke, M. Hermle, W. Warta, and M. C. Schubert, "Efficiency limiting bulk recombination in multicrystalline silicon solar cells," *Solar Energy Materials and Solar Cells*, vol. 98, pp. 441–447, 2012.